Available online at www.sciencedirect.com
SCIENCE DIRECT®
Journal of Organometallic Chemistry 690 (2005) 1814–1821
Journal of Organometallic Chemistry
www.elsevier.com/locate/jorganchem

Nickel(II) bis(diphenylphosphino)amide: Redox-coupling of dppa ligands in coordination sphere of Ni^{2+} and some other properties

Vyacheslav V. Sushev [a], Alexander N. Kornev [a,*], Yurii A. Kurskii [a], Olga V. Kuznetsova [a], Georgy K. Fukin [a], Yulia H. Budnikova [b], Gleb A. Abakumov [a]

[a] G.A. Razuvaev Institute of Organometallic Chemistry, Russian Academy of Sciences, 49 Tropinin Street, 603950 Nizhny Novgorod, Russia
[b] A.E. Arbuzov Institute of Organic and Physical Chemistry, Kazan Scientific Centre of the Russian Academy of Sciences, 8 Arbuzov Street, 420088 Kazan, Russian Federation

Received 11 January 2005; accepted 7 February 2005
Available online 17 March 2005

Abstract

The reactions of $Ni^{II}[(PPh_2)_2N]_2$ (**2**) with various reagents are described. Addition of two moles of carbon monoxide to **2**, at 20 °C and atmospheric pressure leads to the redox coupling of dppa ligands and formation of zero-valent nickel complex $(CO)_2Ni(Ph_2P{-}N{=}PPh_2{-}PPh_2{=}NPPh_2)$ (**4**). The nickel atom in **4** has a tetrahedral coordination and is incorporated into the NiP_4N_2 ring adopting a distorted chair conformation with phosphorus–phosphorus bond length 2.2777(5) Å. Contrary to CO, sulphur dioxide reacts with **2** to form simple adduct $(SO_2)Ni^{II}[(PPh_2)_2N]_2$. The reaction of **2** with allyl bromide runs as alkylation of dppa ligand to form All-$N(PPh_2)_2NiBr_2$. The reduction of **2** with metallic sodium in THF gives Ni(0) complex, $HN(PPh_2)_2Ni(Ph_3P)_2$ (**7**). The electrochemical reduction of **2** in CH_2Cl_2 takes place in two steps: reversible one-electron and quasi-reversible three-electron step.

Keywords: Transition metal complexes; Phosphazanes; Phosphinoamides; Amidoimidophosphoranes; X-ray diffraction

1. Introduction

Bis(diphenylphosphino)amine, $HN(PPh_2)_2$, is one of the much used and intriguing phosphorus–nitrogen ligands in transition-metal chemistry [1]. It demonstrates coordinative versatility both in its neutral form and as an anion $[Ph_2PNPPh_2]^-$ (dppa) [2]. Moreover, the last one is implicated easily into redox processes (oxidative splitting and scrambling of the ligand), which usually are accompanied with $P^{III} \rightarrow P^{V}$ transitions. So, the oxidation of lithium bis(diphenylphosphino)amide, $LiN(PPh_2)_2$, (**1**) with molecular iodine affords single, P–P coupled product, $Ph_2P{-}N{=}PPh_2{-}PPh_2{=}N{-}PPh_2$ [3]. On the other hand, **1** reacts with a number of inorganic halides to form unexpected products of cyclophosphazene type $[Ph_2P(NPPh_2)]_2M$ (M = Co [4], Ni, Pd [5]), $[Ph_2P(NPPh_2)]M[(Ph_2P)_2N]$ ($M = Fe^{II}$, Pt^{II}) [6].

$$3MCl_2 + 6LiN(PPh_2)_2 \rightarrow [(Ph_2PN)_2PPh_2]_2M + 2(Ph_2P)_3N + 2M + 6LiCl \quad M = Co, Ni$$

Tris(diphenylphosphino)amine, $(Ph_2P)_3N$, was the main product (55%) in the reaction of germanium dichloride dioxanate with **1** [7,8]. The reaction of $LiN(PPh_2)_2$ with PCl_3, lead to the mixture of cyclic $\{N(Ph_2P{=}P{-}PPh_2)_2N\}$, and linear $\{(Ph_2P{-}N{=}PPh_2{-})_2\}$ phosphazenes [3].

* Corresponding author. Tel.: +78312 12 66 52; fax: +78312 12 74 97.
E-mail address: akornev@imoc.sinn.ru (A.N. Kornev).

0022-328X/$ - see front matter © 2005 Elsevier B.V. All rights reserved.
doi:10.1016/j.jorganchem.2005.02.007

Recently, we have synthesised nickel(II) bis(diphenylphosphino)amide (**2**) in disproportionation reaction of nickel(I) bis(triphenylphosphino)bis(trimethylsilyl)-amide with $(Ph_2P)_2NH$:

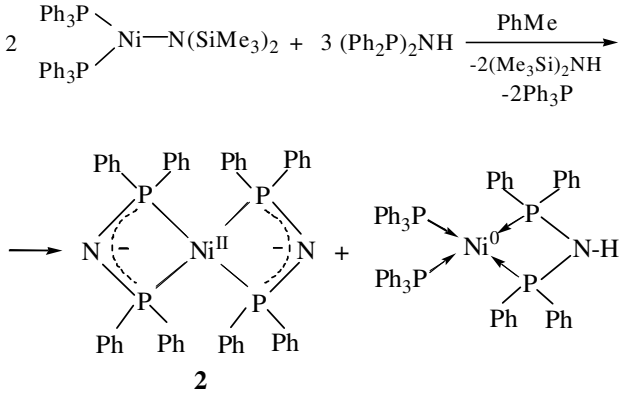

The reaction affords good yield of **2** according stoichiometry of the equation. In this paper we report unusual properties of **2** including oxidative coupling of dppa ligands, the electrochemical and chemical reduction, interaction with SO_2 and allyl bromide, as well as a novel structural investigation of **2**.

2. Results and discussion

Previously, we have shown [9] that central core of nickel(II) bis(diphenylphosphino)amide (**2**) is flat at 150 K. It was revealed further that crystals of **2** being red at room temperature turned yellow at 150 K. The compound has no ^{31}P NMR spectrum at 20 °C. It was reasonable to study the structure of the molecule at room temperature. The X-ray investigation at 293 K has shown however that the structure of the molecule changes marginally. The central core of **2** retains flat geometry. Apparently, the temperature dependent color transition has an electronic nature. It may be the case when small deviation out of plain conformation under change of temperature causes considerable changes in electron levels.

2.1. Reactivity

2.1.1. Interaction with carbon monoxide

A solution of **2** in THF absorbs carbon monoxide (two moles per one mole of **2**) at atmospheric pressure and ambient temperature with the rate of gas diffusion into a solution. The red colour of the solution becomes markedly deeper. The electronic spectrum showed a fast disappearance of absorption bands of the initial complex at 414 nm ($\varepsilon = 80$), 431 nm ($\varepsilon = 660$) while new strong absorption at 403 nm ($\varepsilon = 1350$) arose. Solvent removal led to a brown polycrystalline solid **3**, whose IR spectrum shows two carbonyl bands 1980 and 1920 cm^{-1}, indicating the presence of two CO molecules, coordinated to the nickel atom.

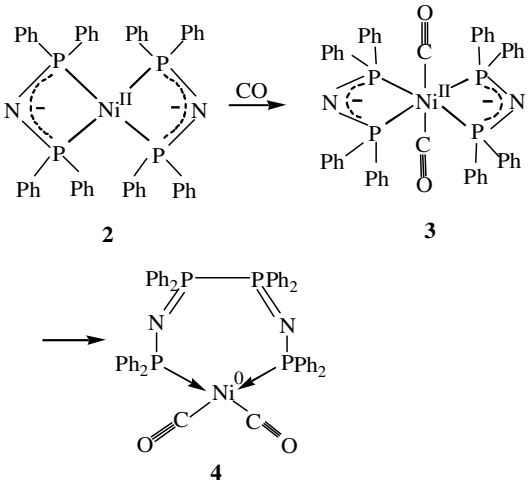

Our attempts to detect the coordination of only one CO-ligand to nickel atom were unsuccessful. The proposed intermediate complex **3** in THF (or CH_2Cl_2) solution undergoes slow (during ~10 h) transformation to the compound **4** (as judged by ^{31}P NMR monitoring). The rearrangement proceeds quite fast (~15 min) when irradiated by soft UV (~330 nm, Pyrex). The absorption band is shifted to 400 nm, and its intensity sharply decreases ($\varepsilon = 330$). The ^{31}P NMR spectrum of **4** corresponds to the AA′XX′ spin system containing two multiplets at 68.0 ppm (P^{III}) and 5.1 ppm (P^{V}). IR spectrum of **4** shows new strong absorptions at 1210 and 1160 cm^{-1}, assigned to the stretching vibrations of the $N{-}P^{V}{=}N$ moiety.

Yellow crystals of **4** suitable for X-ray analysis were prepared from a THF/toluene (1:1) mixture. The X-ray diffraction study of the complex (Fig. 1) showed that the nickel atom has a tetrahedral coordination and is incorporated into the NiP_4N_2 ring adopting a distorted chair conformation. Note that in the similar previously studied platinum complex, $Me_2Pt(PPh_2NPPh_2PPh_2NPPh_2)$ [10], the metal atom has a square-planar environment while the PtP_4N_2 ring adopts a boat conformation. The different conformations of nickel and platinum complexes seem to result from significantly different P(1)–P(4) interatomic distances which are primarily determined by P–M–P bond angles {107.65(2)° for **4** and 94.0(1)° for the platinum complex}.

The Ni(1)–P(1) and Ni(1)–P(4) bond distances are 2.2073(4) and 2.2129(4) Å, respectively; they are shorter than the Pt–P distances (2.283(3), 2.285(3) Å) in the platinum complex $Me_2Pt(PPh_2NPPh_2PPh_2NPPh_2)$ [10]

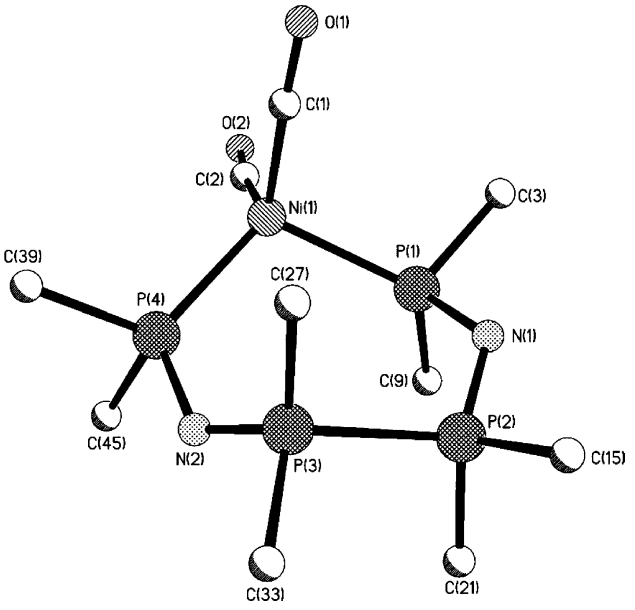

Fig. 1. Molecular structure of **4**. Phenyl rings are omitted for clarity.

and are comparable with similar distances (2.221(1) Å) in $(OC)_2Ni^0(PPh_3)_2$ [11]. Nonetheless, the P(1)–P(4) distance between the phosphorus atoms bound to nickel in compound **4** is 3.568(1) Å, which is substantially longer than the same distance in the Pt complex (3.338(1) Å [10]). Such a difference in P–P distances points to the flexibility of the ligand and its capability to form complexes with metals of different radii.

The P(2)–P(3) distance (2.2777(5) Å) in **4** is markedly longer than that in the free ligand (2.232(2) Å) [3], which adopts a zigzag configuration. In the platinum complexes $Me_2Pt(PPh_2NPPh_2PPh_2NPPh_2)$ and $IMePt(PPh_2NPPh_2$-$PPh_2NPPh_2)$ similar P(2)–P(3) distances are 2.290(4) and 2.242(5) Å, respectively [10]. The P(2)–P(3) bond length is obviously to be determined mainly by the electronic state of a metal and the strength of its bond to phosphorus atom rather than by the ring size. It should be noted that this bond can be readily broken when the free ligand reacts with zerovalent palladium or platinum complexes [10].

$$(Ph_3P)_4M^0 + PPh_2NPPh_2PPh_2NPPh_2 \rightarrow [N(PPh_2)_2]_2M^{II} + 4Ph_3P$$

Note that there are shortened intramolecular C···C distances between the phenyl rings in the $–Ph_2P(2)–P(3)Ph_2–$ moieties (3.281(3) Å) in compound **4**, as well as between the carbonyl group and phenyl ring (3.302(3) Å) as compared with normal van der Waals contacts C–C, 3.42 Å [12].

The P–N distances in complex **4** may be divided into two groups: formally ordinary bonds, P(1)–N(1) (1.672(1) Å) and P(4)–N(2) (1.657(1) Å), and double bonds, P(2)–N(1) (1.575(1) Å) and P(3)–N(2) (1.570(1) Å), which differ by ~0.1 Å. A similar situation is observed in the Pt complexes [10]. The Ni(1)–C(1, 2) and C(1, 2)–O(1, 2) distances are 1.776(2), 1.763(2) Å and 1.145(2), 1.147(2) Å, which is close to the corresponding Ni–C (1.763(2) Å) and C–O (1.142(3) Å) distances in $(OC)_2Ni^0(PPh_3)_2$ [13].

Discussing the rearrangement it is necessary to recollect another interesting example of related Ni(II) → Ni(0) conversion. So chelating nickel(II) phosphineamide complex reacts with carbon monoxide to generate new product in which C–N reductive coupling has taken place [14]:

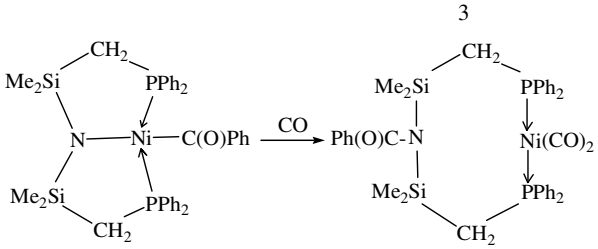

*2.1.1.1. Solubility of **2** and crystal growth.* Nickel(II) bis(diphenylphosphino)amide (**2**) shows unusual solubility in different solvents. It is easily soluble in CH_2Cl_2 (UV/vis spectroscopy shows single transition at 450 nm), but reacts with $CHCl_3$ for 1 h to form insoluble red product. THF can dissolve **2**, however the formation of red solution takes heating for a long time (~4 h). Recovering of **2** from THF or CH_2Cl_2 solution gave unchangeable product as judged by IR spectroscopy. Initial addition of MeCN to crystals of **2** causes its immediate dissolution, however a brown-yellow precipitate is formed soon. Subsequent addition of acetonitrile results in complete dissolution of last one. Interestingly, this solution does not absorb CO at ambient conditions. The observed behavior of **2** may be the result of double-sided basket-like structure, which may delay equilibrium coordination of the solvent molecules. Note that crystallization of known Ni(II) complex, containing neutral bis(diphenylphosphino)metane ligand (dppm)-$[Ni(dppm)_2](BF_4)_2$, from acetonitrile, gave five-coordinate compound $[Ni(dppm)_2(MeCN)](BF_4)_2$ [15].

*2.1.2. Interaction of **2** with sulfur dioxide*

It was found that solution of nickel(II) bis(diphenylphosphino)amide in THF easily absorbs one equivalent of sulfur dioxide to form insoluble yellow fine-crystalline powder of **5**. The efficient magnetic moment observed for **5** (2.3 μ_B) revealed Ni^{2+} oxidation state. So, there are no coupling of dppa ligands took place in this case. The infrared spectrum of **5** showed $\nu(SO_2)$ peaks at: 1200 (m), 1130 (vs), 1100 (m), 1030 (m) cm^{-1}. The vibrational frequencies of the SO_2 ligand

in **5** are in the range established for those nickel complexes, which contain the pyramidal $NiSO_2$ geometry [16].

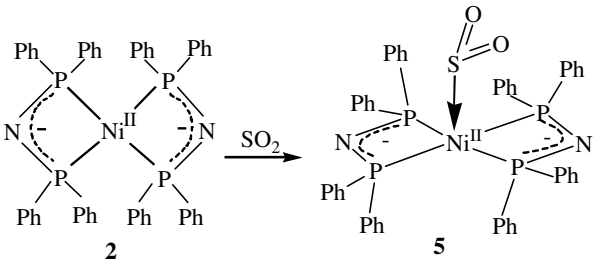

It is known that sulfur dioxide forms charge-transfer complexes with tetrtiary amines [17]. So, the formation of $^{-}O–S(O)–N(PPh_2)_2Ni^{+2}$ moiety is also possible. Note, however, that such a charge division will be energetically unfavourable; furthermore, an excess of SO_2 gave the same product, containing one SO_2 molecule per nickel atom according element analysis. Therefore, the coordination of SO_2 to the nickel atom is more probable.

2.1.3. Reaction of **2** with allyl bromide

The reaction of **2** with excess of allyl bromide proceed smoothly to form deep red solution. Keeping this solution at room temperature gives wine-red crystals of new complex **6**.

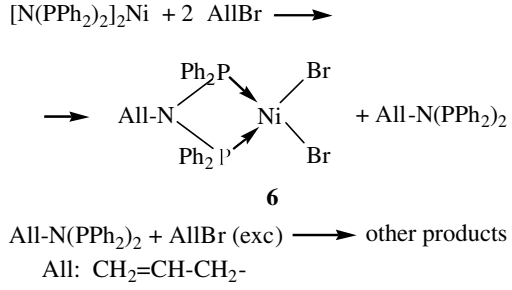

The ^{31}P NMR spectrum of **6** contains single resonance at 51.7 ppm. X-ray analysis has shown that the Ni(II) atom has a distorted square-planar coordination (Fig. 2). The Ni(1)–P(1)N(1)–P(2) metallocycle is also planar. The bromine atoms occupy a *trans*-positions relatively of the Ni(1)–P(1)N(1)–P(2) metallocycle. The deviations of Br(1) and Br(2) atoms from the Ni(1)–P(1) P(2) plain are +0.341 Å and −0.186 Å, respectively. The Ni (1)–P(1,2); Ni(1)–Br(1,2) and N(1)–P(1,2) distances are 2.112(1), 2.122(2) Å; 2.321(1), 2.319(1) Å and 1.692(4), 1.709(4) Å, respectively. In the similar known complex, $MeN[(o\text{-}Pr^iC_6H_4)_2P]_2NiBr_2$ [18], only the Ni–P (2.161 Å) distances are elongated due to steric hindrances as compared to the Ni–P distances in **6** while the Ni–Br (2.328 Å) and N–P (1.688 Å) distances are close to the analogous bond lengths in **6**. The allyl fragment C(25)–C(26)–C(27) is planar. The C(25)–C(26) and C(26)–C(27) distances are 1.484(8) and 1.310(7) Å. These distances are close to a typical $C(sp^3)–C(sp^2)$ (1.503 Å) and $C(sp^2)–C(sp^2)$ (1.299 Å) bond lengths in the $C{-}CH{=}CH_2$ fragments [19]. The distance N(1)–C(25) 1.477(6) Å is close to the analogous bond length in $MeN[(o\text{-}Pr^iC_6H_4)_2P]_2NiBr_2$ (1.474 Å [18]). The deviation of C(25) atom from the plane of the cycle Ni(1)–P(1)–N(1)–P(2) is (0.298 Å). The dihedral angle between C(25)–C(26)–C(27) and Ni(1)–P(1)–N(1)–P(2) planes is 84.0° (see Fig. 2).

High reactivity of **2** toward allyl bromide may be result of essential negative charge of nitrogen atoms. The mother liquor, remaining after crystallization of **6**, was monitored by ^{31}P NMR spectroscopy. The observed single resonance at δ 24.0 ppm is not in contradiction with the presence of allylbis(diphenylphosphino)amine $CH_2{=}CH{-}CH_2{-}N(PPh_2)_2$ (the second product of the reaction). Maintaining of this solution for a long time gave more complicated mixture of phosphorus-containing products, according to the ^{31}P NMR spectroscopy.

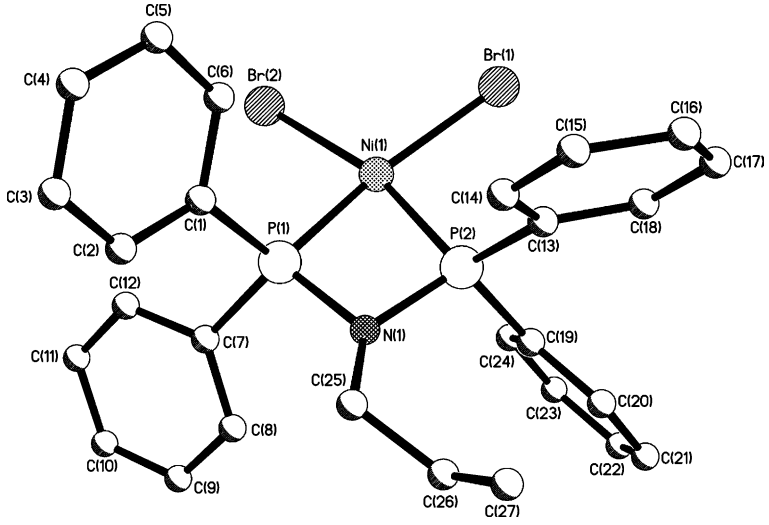

Fig. 2. Molecular structure of $All\text{-}N(PPh_2)_2NiBr_2$ (**6**).

It worth note that methylation of dppa derivatives of platinum and palladium with methyl ether of fluorosulphonic acid proceed in analogous way [20]:

$$M(dppa)_2 + CH_3OSO_2F \rightarrow \{[CH_3N(PPh_2)_2]_2M\}^{2+}(^{-}OSO_2F)_2 \quad M = Pt, Pd$$

2.1.4. Reduction of **2**

Since compound **2** contains divalent nickel, it may be reduced to Ni^{+1} or Ni^0 state. The electrochemical reduction of **2** occurs by two steps. The primary electron-transfer step is reversible one-electron process (Fig. 4). The second step is quasi-reversible three-electron reduction. Obviously, the second step touches dppa-ligand itself along with metallocentre. Eventually, it results in destruction of the complex.

The interaction of **2** with metallic sodium in THF at 20 °C proceeds slowly to form dark-brown solution and no tractable products. Meanwhile, addition of equivalent amounts of Ph_3P to this solution and subsequent crystallization from ether affords large dark-brown crystals of Ni(0) mixed-ligand complex $HN(PPh_2)_2$-$Ni(Ph_3P)_2$ (**7**). The ^{31}P NMR spectrum of **7** corresponds to the AA′XX′ spin system containing two triplets at δ 61.9 and 33.5 ppm with splitting constant $^2J_{PP}$ 20.3 Hz.

The X-ray diffraction data has shown that the Ni(1) atom has a distorted tetrahedral coordination (4). The Ni(1)–P(1,2) distances 2.1983(5), 2.2006(5) Å are slightly longer than the Ni(1)–P(3,4) (2.1842(5), 2.1875(5) Å) distances. This is indicative of weaker dppa coordination to nickel atom by comparison with Ph_3P ligand. At the same time the distances Ni(1)–P(1,2) are much elongated as compared to Ni^{2+}–P distances in **6** {2.112(1), 2.122(2) Å} and the Ni^{2+}–P distances in $MeN[(o\text{-}Pr^iC_6H_4)_2P]_2NiBr_2$ (2.161 Å [18]). The nitrogen–phosphorus bond lengths in **7** {1.705(1), 1.698(1) Å} are very close to similar N–P distances in **6** (1.692(4), 1.709(4) Å) and in $MeN[(o\text{-}Pr^iC_6H_4)_2P]_2$-$NiBr_2$ (1.688 Å [18]). The Ni–P co-ordination bond strength is revealed also in the observed PNP bond angles which are increased on going from Ni^{2+} to Ni^0 complexes: 94.3(2)° in **6** (Ni^{2+}), 100.98° in $MeN[(o\text{-}Pr^iC_6H_4)_2P]_2NiBr_2$ (Ni^{2+}) and 102.21(8)° in **7** (Ni^0). The dihedral angle between the planes of Ni(1)–P(1)–N(1)–P(2) and Ni(1)–P(3)–P(4) fragments in **7** are 81.5°, that apparently minimizes steric repulsion of Ph groups of Ph_3P and dppa ligands.

Obviously, the formation of **7** is not possible without hydrogen abstraction from the solvent.

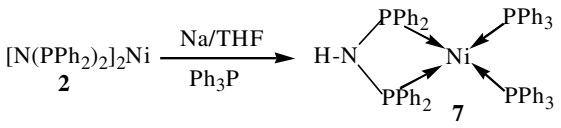

It worth noting, bis(cyclopentadienyl)cobalt being strong reducing agent, does not react with **2** in THF solution, perhaps due to steric hindrances.

3. Experimental

3.1. General considerations

Solvents were purified following standard methods [21]. Toluene and methylene chloride were thoroughly dried and distilled over P_2O_5 prior to use. Ether and THF were dried and distilled over Na/benzophenone.

Bis(diphenylphosphino)amine, $(Ph_2P)_2NH$, was prepared according to [22]. All manipulations were performed with rigorous exclusion of oxygen and moisture, in vacuum or under an argon atmosphere using standard Schlenk techniques. An CO and SO_2-gas was dried over phosphorus(V) oxide.

Spectrophotometric determination of nickel with dimethylglioxime was provided by the method [23];

Infrared spectra were recorded on a Perkin–Elmer 577 spectrometer from 4000 to 400 cm^{-1} in Nujol.

NMR spectra were recorded in $CDCl_3$ or C_6D_6 solutions using "Bruker DPX-200" device, with Me_4Si as internal standard.

Cyclic voltammograms were recorded at glassy carbon electrode with a 1.5 mm diameter in a thermostatically controlled cell in argon atmosphere. Silver electrode $Ag/AgNO_3$ (0.01 mol l^{-1} solution in MeCN) served as a reference electrode and platinum wire served as an auxiliary electrode. Curve registration was performed with potentiostat PI-50-1 (USSR). Scan rate was 50 mV s^{-1} (Fig. 3).

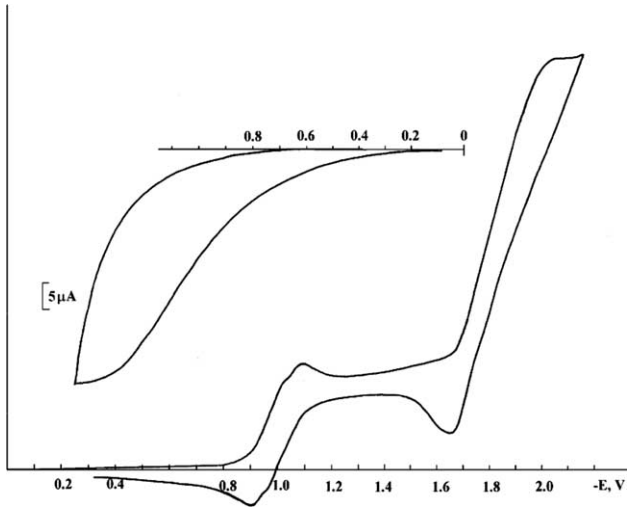

Fig. 3. Cyclic voltammograms for $Ni^{II}[(PPh_2)_2N]_2$ (**2**) (5×10^{-3} M) in $CH_2Cl_2 + Et_4NBF_4$ (10^{-1} M).

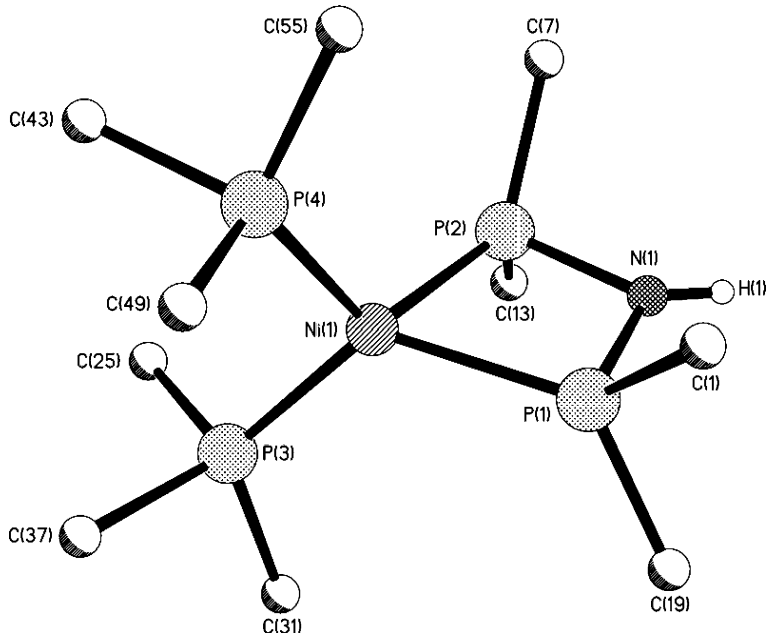

Fig. 4. Molecular structure of $HN(PPh_2)_2Ni(Ph_3P)_2$ (**7**). Phenyl rings are omitted for clarity.

Table 1
The details of crystallographic, collection and refinement data for **4**, **6** and **7**

	4	**6**	**7**
Empirical formula	$C_{50}H_{40}N_2NiO_2P_4$	$C_{27}H_{25}Br_2NNiP_2$	$C_{62}H_{56}NNiO_{0.5}P_4$
Formula weight	883.43	643.95	1005.67
Temperature (K)	100(2)	100(2)	100(2)
Crystal system	Monoclinic	Monoclinic	Monoclinic
Space group	$P2_1/n$	$P2_1/n$	$P2_1/n$
Unit cell dimensions			
a (Å)	13.7895(9)	10.4261(12)	11.6497(11)
b (Å)	22.7483(15)	19.107(2)	36.480(3)
c (Å)	13.9372(9)	13.1969(15)	12.2311(11)
β (°)	98.4310(10)	99.234(2)	92.563(2)
V (Å)^3	4324.7(5)	2594.9(5)	5192.8(8)
Z	4	4	4
D_{calc} (g/cm^3)	1.357	1.648	1.286
Absorption coefficient (mm^{-1})	0.640	3.967	0.539
$F(000)$	1832	1288	2108
Crystal size (mm^3)	$0.30 \times 0.20 \times 0.20$	$0.40 \times 0.30 \times 0.20$	$0.40 \times 0.40 \times 0.40$
θ Range for data collection (°)	1.74–29.02	1.89–29.05	1.76–25.00
Index ranges	$-18 \leqslant h \leqslant 18$	$-11 \leqslant h \leqslant 14$	$-13 \leqslant h \leqslant 13$
	$-18 \leqslant k \leqslant 30$	$-26 \leqslant k \leqslant 20$	$-43 \leqslant k \leqslant 43$
	$-18 \leqslant l \leqslant 18$	$-17 \leqslant l \leqslant 18$	$-14 \leqslant l \leqslant 14$
Reflections collected	31 151	18 702	36 415
Independent reflections [R_{int}]	11 425 [0.0240]	6880 [0.0912]	9146 [0.0321]
Absorption correction	SADABS		
Maximum/minimum transmission	0.8828/0.8313	0.5042/0.2998	0.8134/0.8134
Refinement method	Full-matrix least-squares on F^2		
Data/restraints/parameters	11425/0/692	6880/0/298	9146/10/644
Goodness-of-fit on F^2	1.042	0.923	1.069
Final R indices [$I > 2\sigma(I)$]	$R = 0.0344$,	$R = 0.0520$	$R = 0.0332$
	$R_w = 0.0861$	$R_w = 0.0876$	$R_w = 0.0827$
R indices (all data)	$R = 0.0452$,	$R = 0.1204$	$R = 0.0377$
	$R_w = 0.0920$	$R_w = 0.1061$	$R_w = 0.0846$
Largest difference in peak and hole (e Å^3)	0.605/−0.306	0.916/−1.143	0.533/−0.227

Table 2
The selected distances (Å) and angles (°) for **4**, **6** and **7**

4		**6**		**7**	
Bond distance (Å)					
Ni(1)–P(1)	2.2073(4)	Ni(1)–Br(1)	2.3212(7)	Ni(1)–P(1)	2.1983(5)
Ni(1)–P(4)	2.2129(4)	Ni(1)–Br(2)	2.319(1)	Ni(1)–P(2)	2.2006(5)
Ni(1)–C(1)	1.776(2)	Ni(1)–P(1)	2.112(1)	Ni(1)–P(3)	2.1842(5)
Ni(1)–C(2)	1.763(2)	Ni(1)–P(2)	2.122(2)	Ni(1)–P(4)	2.1875(5)
P(1)–N(1)	1.672(1)	P(1)–N(1)	1.692(4)	N(1)–P(1)	1.705(1)
P(2)–N(1)	1.575(1)	P(2)–N(1)	1.709(4)	N(1)–P(2)	1.698(1)
P(4)–N(2)	1.657(1)	N(1)–C(25)	1.477(6)		
P(3)–N(2)	1.570(1)	C(25)–C(26)	1.484(8)		
O(1)–C(1)	1.145(2)	C(26)–C(27)	1.310(7)		
O(2)–C(2)	1.147(2)				
Bond angles (°)					
C(2)–Ni(1)–C(1)	108.38(7)	P(1)–Ni(1)–P(2)	73.77(5)	P(3)–Ni(1)–P(4)	108.18(2)
C(2)–Ni(1)–P(1)	103.60(5)	P(1)–Ni(1)–Br(2)	93.09(5)	P(3)–Ni(1)–P(1)	124.00(2)
C(1)–Ni(1)–P(1)	105.38(5)	P(2)–Ni(1)–Br(2)	166.20(4)	P(4)–Ni(1)–P(1)	115.40(2)
C(2)–Ni(1)–P(4)	116.55(5)	P(1)–Ni(1)–Br(1)	164.61(5)	P(3)–Ni(1)–P(2)	111.05(2)
C(1)–Ni(1)–P(4)	114.16(5)	P(2)–Ni(1)–Br(1)	93.49(4)	P(4)–Ni(1)–P(2)	121.37(2)
P(1)–Ni(1)–P(4)	107.65(2)	Br(2)–Ni(1)–Br(1)	100.12(3)	P(1)–Ni(1)–P(2)	74.02(2)
N(1)–P(1)–Ni(1)	121.14(5)	N(1)–P(1)–Ni(1)	95.2(1)	P(2)–N(1)–P(1)	102.21(8)
P(2)–N(1)–P(1)	127.63(8)	N(1)–P(2)–Ni(1)	94.3(2)		
N(2)–P(3)–P(2)	114.21(5)	P(1)N(1)–P(2)	96.7(2)		
P(3)–N(2)–P(4)	130.88(9)	N(1)–C(25)–C(26)	112.7(4)		
N(2)–P(4)–Ni(1)	119.54(5)	C(27)–C(26)–C(25)	123.3(5)		
O(1)–C(1)–Ni(1)	172.8(2)				
O(2)–C(2)–Ni(1)	173.3(2)				

3.2. X-ray structure determinations

The X-ray diffraction data were collected on a SMART APEX diffractometer (graphite-monochromated, Mo Kα-radiation, φ–ω-scan technique, λ = 0.71073 Å). The intensity data were integrated by SAINT program [24]. SADABS [25] was used to perform area-detector scaling and absorption corrections. The structures were solved by direct methods and were refined on F^2 using all reflections with SHELXTL package [26]. All non-hydrogen atoms were refined anisotropically. All H atoms in **4** were found from Fourier synthesis and refined isotropically. The H atoms in **6** and **7** were placed in calculated positions and refined in the "riding-model" except the H(1) atom in **7** which was found from Fourier synthesis and refined isotropically. The complex **7** contains a disordered solvate molecule of Et_2O. The details of crystallographic, collection and refinement data for **4**, **6** and **7** are shown in the Table 1. The selected distances and bond angles for **4**, **6** and **7** are shown in the Table 2.

3.3. Synthesis

3.3.1. Interaction of 2 with CO, synthesis of $(CO)_2Ni(Ph_2P{-}N{=}PPh_2{-}PPh_2{=}N{-}PPh_2)$ (4)

A Pyrex ampoule containing 0.41 g (0.5 mmol) of **2** in 15 mL of toluene was attached to a mercury burette with carbon monoxide. Absorption of 22.4 mL (1.0 mmol) of CO was occurred for about 30 s. Red solution immediately turned dark violet-brown. The electronic spectrum shows band at 403 nm (ε = 1350). An aliquot part was separated; the solvent was removed in vacuum; remaining brown powder (**2**), was analyzed by IR spectroscopy: 1980 (s), 1920 (s), 1430 (m), 1100 (s), 910 (s), 870 (m), 740 (m), 700 (s), 550 (w), 520 (w), 500 (w).

The ampoule was irradiated with UV lamp of low pressure for 20 min. The yellow solution was concentrated. Crystals of **4** were obtained from THF/toluene (1:1) mixture. Yield 0.37g (85%). Anal. Calc. for $C_{50}H_{40}N_2NiO_2P_4$: C, 67.98; H, 4.56; Ni, 6.64. Found: C, 68.32; H, 4.48; Ni, 6.60%. IR (Nujol) ν(cm^{-1}): 3060 (w), 1980 (vs), 1920 (vs), 1590 (w), 1430 (s), 1300 (ww), 1210 (vs), 1160 (sh), 1100 d (m), 1030 (w), 1000 (w), 750 (s), 700 (s), 530 (sh), 520 (s), 490 (m), 440 (m). $^{31}P\{^1H\}$ NMR ($CDCl_3$), δ 68.0 (P^{III}, m, AA′); 5.1 (P^V, m, XX′); $^2J_{AX} + {}^3J_{AX'} = 39.7$ Hz, $^1J_{X,X'} = \pm 85.0$, $^2J_{AX} = \pm 53.5$, $^3J_{AX'} + {}^4J_{A'X'} = \pm 13.5$; $^2J_{A,A'} = \pm 11.0\}$.

3.3.2. Interaction of 2 with SO_2

An excess of SO_2 (33.6 mL, 1.5 mmol) was added to a solution of **2** (0.41 g, 0.5 mmol) in THF at ambient conditions. A yellow fine-crystalline precipitate of **5** was formed immediately. The precipitate was filtered, washed with THF and dried in vacuum. Yield 0.39 g (88%). Anal. Calc. for $C_{48}H_{40}P_4N_2NiSO_2$: C, 64.67; H,

4.52; Ni, 6.58; S, 3.60. Found: C, 64.61; H, 4.48; Ni, 6.63; S, 3.54%. IR (Nujol) ν (cm^{-1}): 1200 (m), 1180 (w), 1130 (vs), 1100 (m), 1070 (w), 1030 (m), 1000 (m), 920 (m), 820 (m), 750 (s), 720 (s), 700 (vs), 560 (s), 510 (s). $\mu_{eff} = 2.3\ \mu_B$.

*3.3.3. All-N(PPh_2)$_2$$NiBr_2$ (**6**)*

An excess of allyl bromide (2 mL) was added to 0.3 g of **2**. Red-cerise solution was kept at 20 °C for 3 h. During this time dark red-cerise crystals of **5** were formed. Crystals were separated by filtration, washed with toluene and dried in vacuum. Yield 0.20 g (85%). ^{31}P {^1H} NMR ($CDCl_3$): δ 51.6 ppm; ^1H NMR δ 8.3–7.4 (m, 20H, Ph); 5.25 (m, 1H, —CH═); 4.83 (m, 1H, CH_2═); 4.76 m, 1H (CH_2═); 3.38 (m, 2H, –CH_2–). Anal. Calc. for $C_{27}H_{25}Br_2NNiP_2$: C, 50.36; H, 3.91; Ni, 9.12; Br, 24.82. Found: C, 50.45; H, 4.05; Ni, 9.04; Br, 24.13%. IR (Nujol) ν (cm^{-1}): 1430 (w), 1170 (w), 1110 (s), 1010 (m), 940 (w), 830 (m), 760 (m), 730 (w), 700 (s), 600 (w), 570 (m), 520 (s). NMR-monitoring of mother liquor showed signal ^{31}P δ 24.0 ppm, which may be tentatively refer to allyldiphenylphosphine.

*3.3.4. Interaction of **2** with metallic sodium*

The reaction of **2** (0.27 g, 0.33 mmol) with an excess of sodium metal in THF (10 mL) at 20 °C proceeds slowly (24 h) to form bright-orange then dark-brown solution. The solution was decanted, THF was changed for diethyl ether and 0.2 g of Ph_3P (0.76 mmol) was added. Keeping the mixture overnight at 10 °C affords large dark-brown crystals of Ni(0) mixed-ligand complex $HN(PPh_2)_2Ni(Ph_3P)_2(Et_2O)_{0.5}$ (**7**). Yield 0.14 g (41%). IR (nujol) (cm^{-1}): 3050 w, 1580 w, 1430 m, 1300 m, 1200 m, 1180 m, 1120 m, 1090 s, 1070 w, 1020 m, 790 m, 730 s, 700 vs, 550 m, 510 vs. ^{31}P NMR (C_6D_6), δ ppm: 61.9 (t, $^2J_{PP}$ 20.3, Ph_2P), 33.5 (t, $^2J_{PP}$ 20.3, Ph_3P), ^1H NMR: 2.2 (s, 1H, NH), 6.3–8.1 (m, 50H).

4. Supplementary material

The CIF are available from the Cambridge Crystallographic Data Center under the depositary numbers 259320 (**4**), 259321 (**6**), 259322 (**7**).

Acknowledgements

We are grateful to the Russian Foundation for Basic Research (Grants 03-03-32051, 04-03-32830; scientific schools 1649.2003.3, 1652.2003.3) for financial support of this work.

References

[1] P. Bhattacharyya, J.D. Woollins, Polyhedron 14 (1995) 3367.
[2] M. Witt, H.W. Roesky, Chem. Rev. 94 (1994) 1163.
[3] P. Braunstein, R. Hasselbring, A. Tiripicchio, F. Ugozzoli, J. Chem. Soc. Chem. Comm. (1995) 37.
[4] J. Ellerman, J. Sutter, F.A. Knoch, M. Moll, Angew. Chem., Int. Ed. Engl. 32 (1993) 700.
[5] J. Ellerman, J. Sutter, C. Schelle, F.A. Knoch, M. Moll, Z. Anorg. Allg. Chem. 619 (1993) 2006.
[6] J. Ellerman, P. Gabold, C. Schelle, F.A. Knoch, M. Moll, W. Bauer, Z. Anorg. Allg. Chem. 621 (1995) 1832.
[7] Ya.V. Fedotova, A.N. Kornev, V.V. Sushchev, Yu.A. Kurskii, G.K. Fukin, G.A. Abakumov, Doklady Chem. 396 (1) (2004) 92.
[8] A.N. Kornev, Ya.V. Fedotova, V.V. Sushev, G.K. Fukin, G.A. Abakumov, Amidophosphine derivatives of germanium (II), in: VII International Conference on the Chemistry of Carbenes and Related Intermediates, Book of Abstracts, Kazan, Russia, 23–26 June, 2003, p. 93 {here (P41) means poster 41}.
[9] V.V. Sushev, A.N. Kornev, Y.V. Fedotova, Y.A. Kursky, T.G. Mushtina, G.A. Abakumov, L.N. Zakharov, A.L. Rheingold, J. Organometal. Chem. 676 (2003) 89.
[10] A.M.Z. Slawin, M.B. Smith, J.D. Woollins, J. Chem. Soc., Dalton Trans. (1997) 3397.
[11] C. Kruger, Y.-H. Tsay, Cryst. Struct. Commun. 3 (1974) 455.
[12] Yu.V. Zefirov, P.M. Zorky, Rus. Chem. Rev. l64 (1995) 415.
[13] C. Kruger, Y.-H. Tsay, Cryst. Struct. Commun. 3 (1974) 455.
[14] M.D. Fryzuk, P.A. MacNeil, S.J. Rettig, J. Organometal. Chem. 332 (1987) 345.
[15] A. Miedaner, R.C. Haltiwanger, D.L. DuBois, Inorg. Chem. 30 (1991) 417.
[16] D.C. Moody, R.R. Ryan, Inorg. Chem. 18 (1979) 223.
[17] J.J. Oh, M.S. LaBarge, J. Matos, J.W. Kampf, K.W. Hillig II, R.L. Kuczkowski, J. Am. Chem. Soc. 113 (1991) 4732.
[18] N.A. Cooley, S.M. Green, D.F. Wass, K. Heslop, A.G. Orpen, P.G. Pringle, Organometallics 20 (2001) 4769.
[19] F.H. Allen, O. Kennard, D.G. Watson, L. Brammer, A.G. Orpen, R. Taylor, J. Chem. Soc. Perkin Trans. II. 12 (1987) 1.
[20] H. Schmidbaur, S. Lauteschlager, B. Milewski-Mahrla, J. Organomet. Chem. 254 (1983) 59.
[21] D.D. Perrin, W.L.F. Armarego, D.R. Perrin, Purification of Laboratory Chemicals, Pergamon, Oxford, 1980.
[22] H. Noth, L. Meinel, Z. Anorg. Allg. Chem. 349 (1967) 225.
[23] E. Upor, M. Mohai, Gy. Novak, Photometric Methods in Inorganic Trace Analysis, Academiai Kiado, Budapest, 1985.
[24] Bruker, SAINTPLUS Data Reduction and Correction Program v. 6.02a, Bruker AXS, Madison, WI, USA, 2000.
[25] G.M. Sheldrick, SADABS V.2.01, Bruker/siemens Area Detector Absorption Correction Program, Bruker AXS, Madison, WI, USA, 1998.
[26] G.M. Sheldrick, SHELXTL V. 6.12, Structure Determination Software Suite, Bruker AXS, Madison, WI, USA, 2000.